Camera Specification

BASLER A102f

**Measurement protocol using the
EMVA Standard 1288**

1288
EMVA Standard Compliant

2nd November 2006

BASLER
VISION TECHNOLOGIES

Contents

1 Overview

Basler A102f					
Item	Symbol	Typ.[1]	Std. dev.[2]	Unit	Remarks
Temporal Noise Parameters					
Total quantum efficiency (QE)	η	54	TBD	%	$\lambda = 545\,\mathrm{nm}$
Inverse of overall system gain	$\frac{1}{K}$	4.7	0.08	$\frac{\mathrm{e}^-}{\mathrm{DN}}$	
Temporal dark noise	σ_{d_0}	9	0.4	e^-	
Saturation capacity	$\mu_{e.sat}$	19000	300	e^-	
Spatial Noise Parameters					
Spatial offset noise, DSNU$_{1288}$	σ_o	1.6	0.1	e^-	
Spatial gain noise, PRNU$_{1288}$	S_g	0.7	0.2	%	
Derived Parameters					
Absolute sensitivity threshold	$\mu_{p.min}$	17	TBD	p$^\sim$	$\lambda = 545\,\mathrm{nm}$
Dynamic range	DYN$_{out.bit}$	10.9	0.06	bit	

Table 1: Most important specification data

Operating Point		
Item	Symbol	Remarks
Video output format		$12\,\mathrm{bits/pixel(Mono16)}$
Gain		192
Offset		11
Exposure time	T_{exp}	$100.0\,\mu\mathrm{s}\ to\ 22.1\,\mathrm{ms}$

Table 2: Used camera operating point

---

[1]The unit e^- is used in this document as statistical measured quantity.

[2]The standard deviation was calculated from a sampling of 43 cameras.

2   Introduction

This measurement protocol describes the specification of the Basler A102f cameras. The measurement methods are conform to the EMVA Standard 1288, the Standard for Characterization and Presentation of Specification Data for Image Sensors and Cameras (Release A1.03) of the European Machine Vision Association (EMVA) [1].

The most important specification data of the Basler A102f cameras are summarised in the table 1.

3   Basic Information

Basic Information	
Vendor	Basler
Model	A102f
Type of data presented	Typical
Number of samples	43
Sensor	ICX285AL
Sensor type	CCD
Sensor diagonal	Diagonal 11 mm (Type 2/3)
Indication of lens category to be used	C-Mount
Resolution	1392 x 1040 pixel
Pixel width	$6.45\,\mu\mathrm{m}$
Pixel height	$6.45\,\mu\mathrm{m}$
Readout type	Progressive Scan
Transfer type	Interline transfer
Shutter type	-
Overlap capabilities	
Maximum frame rate	$15\,\mathrm{frames/second}$
General conventions	
Interface type	Firewire 1394a

Table 3: Basic Information

3.1   Illumination

3.1.1   Illumination Setup Basler-CameraTestTool

The illumination during the test of one camera was fixed. The drift of the illumination over a long time and after exchange of the lamp is measured by a reference Basler A602fc camera. The reference camera provides an intensity factor which was used to calculate the irradiance for each camera measurement.

Light source		
Wavelength	λ	$545\,\text{nm}$
Wavelength variation	$\Delta\lambda$	$50\,\text{nm}$
f-number	$f_\#$	$8 = 280\,\text{mm}/35\,\text{mm}$

Table 4: Light source

3.1.2   Measurement of the Irradiance

The irradiance was measured using a Radiometer IL1700 from International Light Inc. (Detector: SEL033 #6285; Input optic: W #9461; Filter: F #21487; regular calibration). The accuracy of the Radiometer is specified as $\pm 3.5\%$.

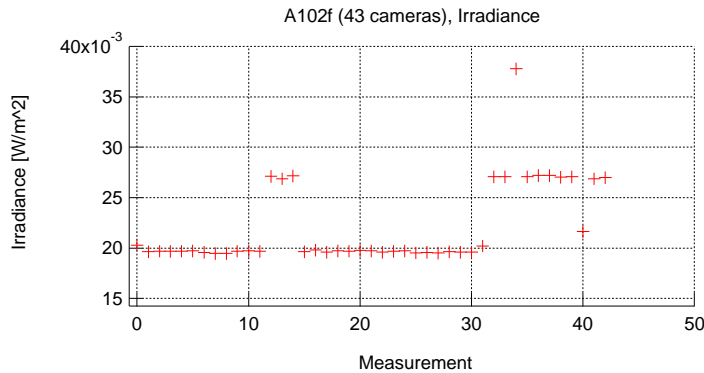   In figure 1 the measured irradiance is plotted.

Figure 1: Irradiance for each camera measurement.

The the error of all calculated values using the amount of light falling on the sensor are dependent of the accuracy of the irradiance measurement.

4 Characterizing Temporal Noise and Sensitivity

4.1 Basic Parameters

4.1.1 Total quantum efficiency

Total quantum efficiency for one fixed wavelenght   Total quantum efficiency $\eta(\lambda)$ in $[\%]$ for monochrome light at $\lambda = 545\,\mathrm{nm}$. With a wavelength variation of $\Delta\lambda = 50\,\mathrm{nm}$.
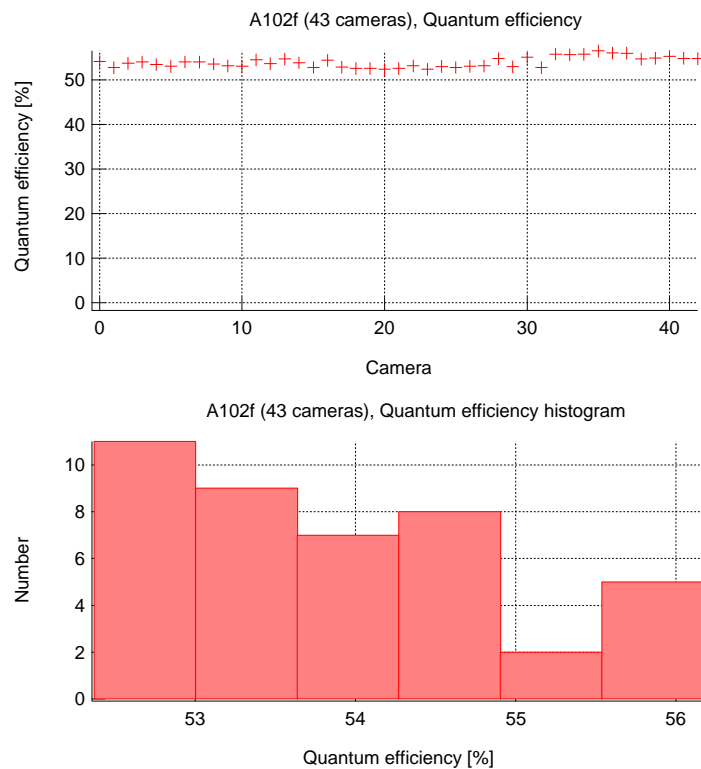
Figure 2: Total quantum efficiency (QE)

Item	Symbol	Typ.	Std. dev.	Unit	Remarks
Total quantum efficiency (QE)	η	54	TBD	$\%$	$\lambda = 545\,\mathrm{nm}$

Table 5: Total quantum efficiency (QE)

The main error of the total quantum efficiency $\Delta\eta$ is related to the error of the measurement of the illumination described in section 3.1.

Total quantum efficiency versus wavelength of the light   Total quantum efficiency $\eta(\lambda)$ in $[\%]$ for monochrome light versus wavelength of the light in $[\mathrm{nm}]$.
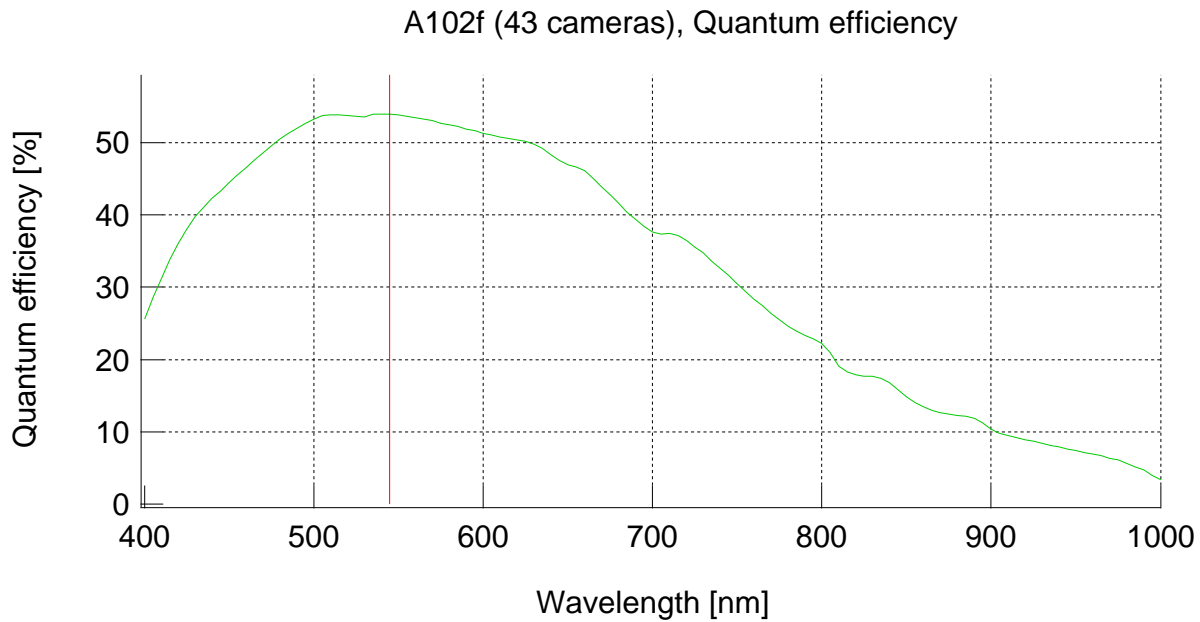

Figure 3: Irradiance for each camera measurement.

The curve of the total quantum efficiency versus the wavelength in figure 3 was calculated from the one measured total quantum efficiency as presented in section 4.1.1. For the shape of the curve the data from the sensor data sheet was used.

4.1.2 Temporal dark noise

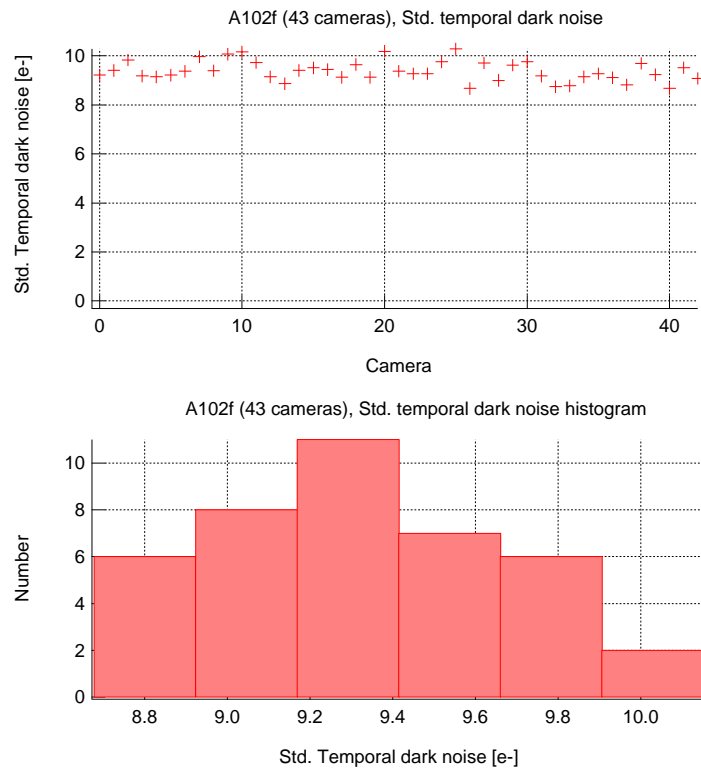Standard deviation of the temporal dark noise σ_{d_0} referenced to electrons for exposure time zero in $[\,\mathrm{e}^-\,]$.

Figure 4: Temporal dark noise

Item	Symbol	Typ.	Std. dev.	Unit	Remarks
Temporal dark noise	σ_{d_0}	9	0.4	e^-	

Table 6: Temporal dark noise

4.1.3   Dark current

Dark current N_{d30} for a housing temperature of $30°\,\mathrm{C}$ in $[\mathrm{e}^-/\mathrm{s}]$.
   Not measured!

4.1.4   Doubling temperature

Doubling temperature k_d of the dark current in $[°\,\mathrm{C}]$.
   Not measured!

4.1.5   Inverse of overall system gain
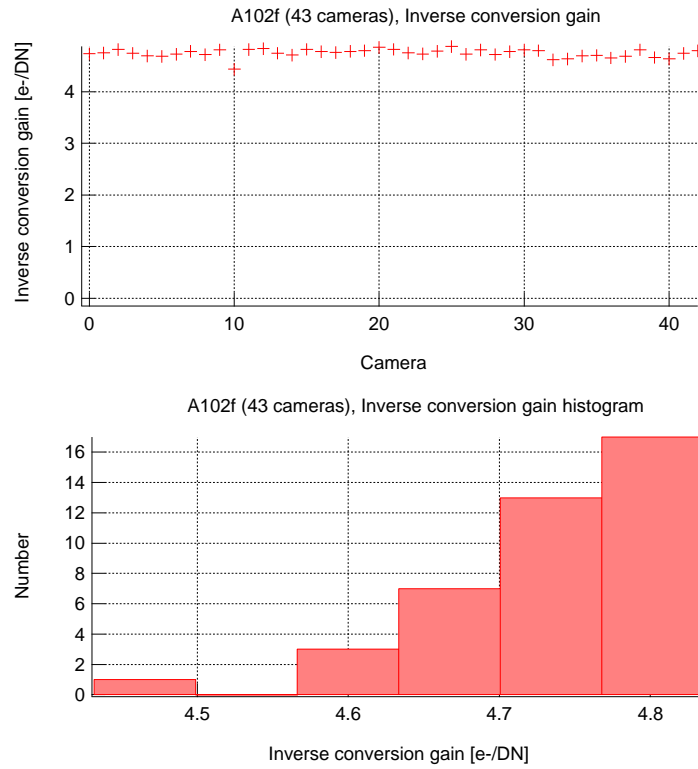
Inverse of overall system gain $\frac{1}{K}$ in $\left[\frac{e^-}{DN}\right]$.

Figure 5: Inverse of overall system gain

Item	Symbol	Typ.	Std. dev.	Unit	Remarks
Inverse of overall system gain	$\frac{1}{K}$	4.7	0.08	$\frac{e^-}{DN}$	

Table 7: Inverse of overall system gain

4.1.6 Inverse photon transfer

Inverse photon transfer $\frac{1}{\eta K}$ in $\left[\frac{\mathrm{p}^{\sim}}{\mathrm{DN}}\right]$.
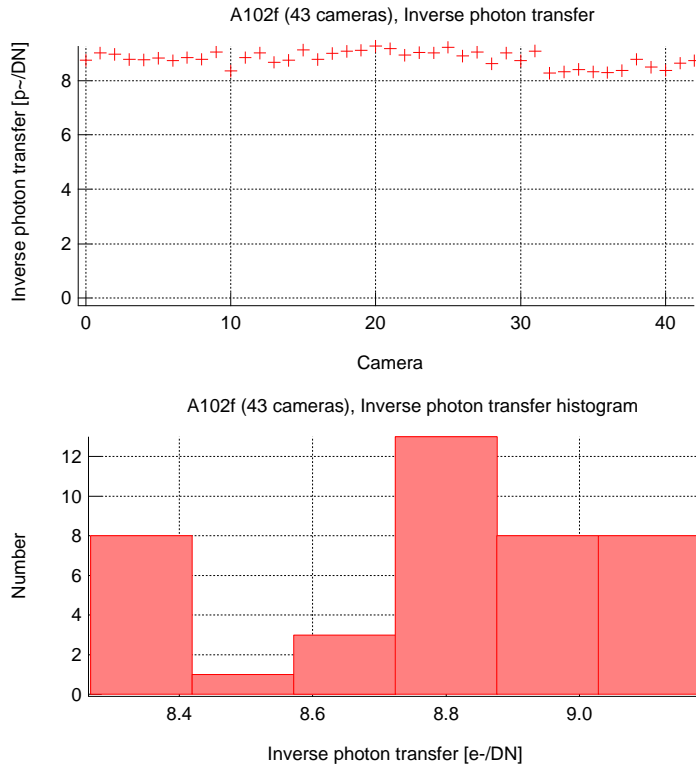

Figure 6: Inverse photon transfer

Item	Symbol	Typ.	Std. dev.	Unit	Remarks
Inverse photon transfer	$\frac{1}{\eta K}$	8.8	TBD	$\frac{\mathrm{p}^{\sim}}{\mathrm{DN}}$	$\lambda = 545\,\mathrm{nm}$

Table 8: Inverse photon transfer

The main error of the inverse photon transfer $\frac{1}{\eta K}$ is related to the error of the measurement of the illumination described in section 3.1.

4.1.7   Saturation capacity

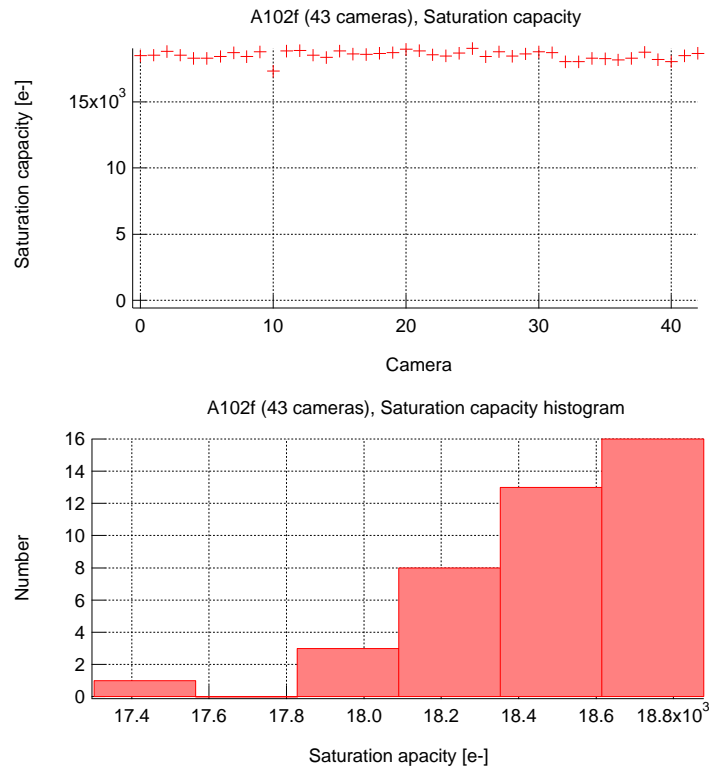Saturation capacity $\mu_{e.sat}$ referenced to electrons in $[\,\mathrm{e}^-]$.

Figure 7: Saturation capacity

Item	Symbol	Typ.	Std. dev.	Unit	Remarks
Saturation capacity	$\mu_{e.sat}$	19000	300	e^-	

Table 9: Saturation capacity

4.1.8   Spectrogram

Spectrogram referenced to photons in $[p^\sim]$ is plotted versus spatial frequency in $[1/\mathrm{pixel}]$ for no light, 50% saturation and 90% saturation.
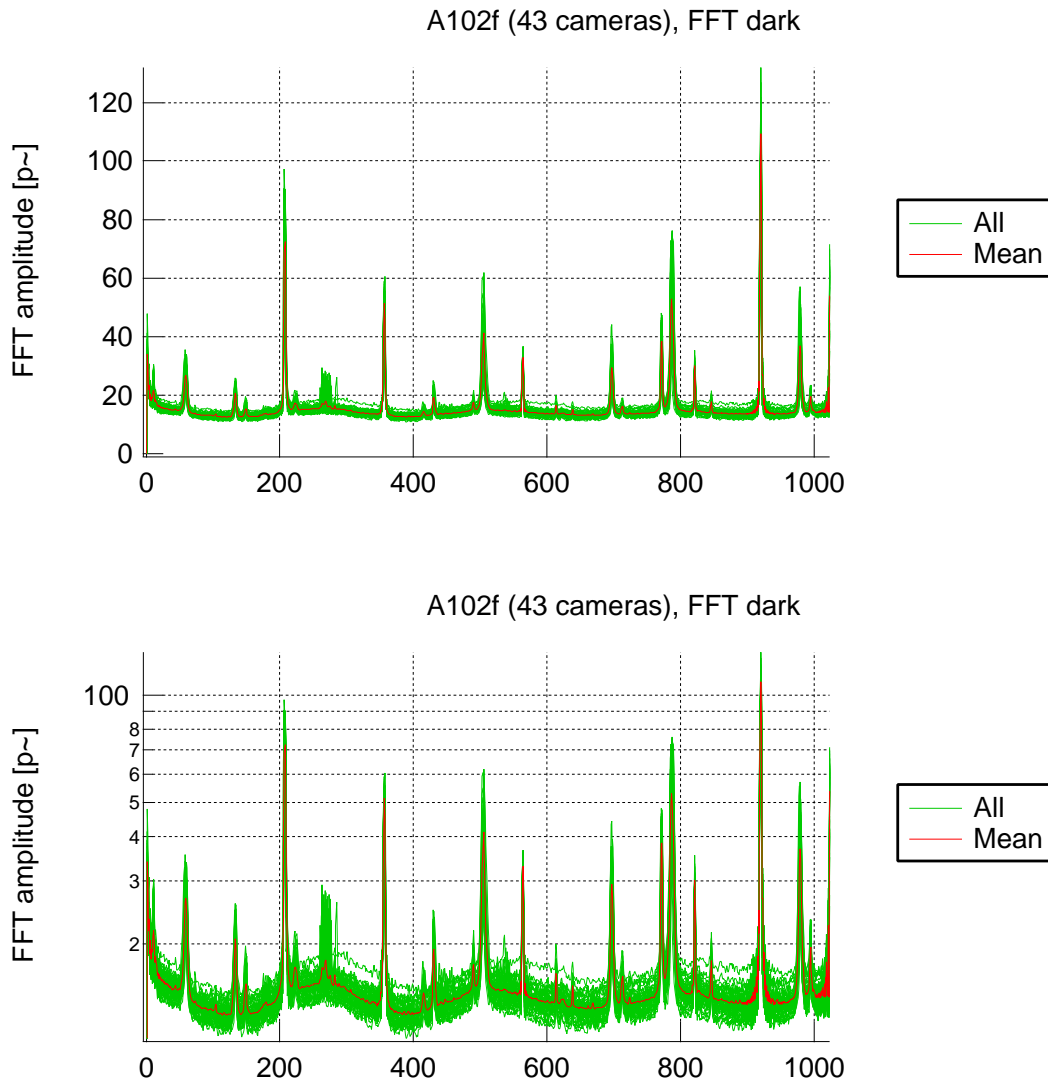

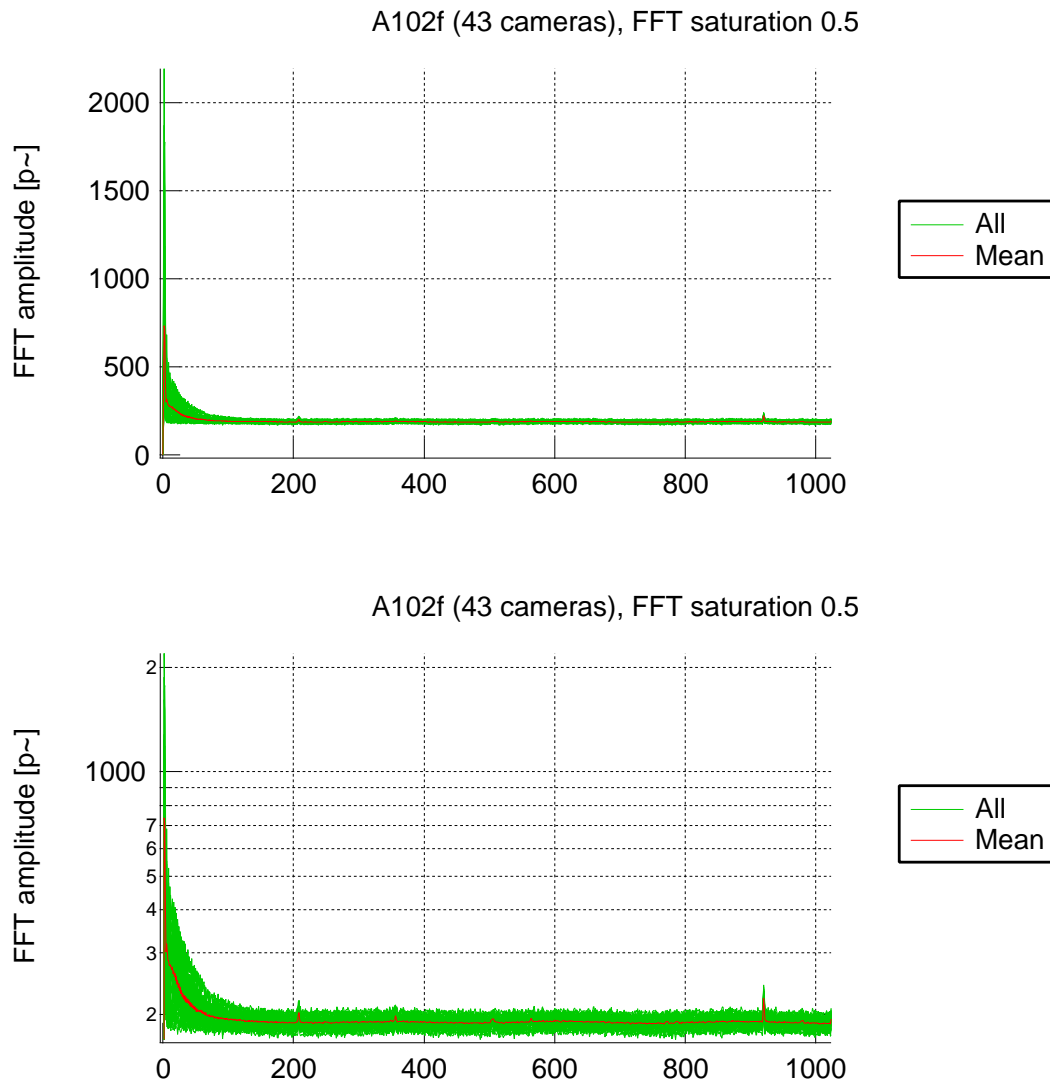Figure 8: Spectrogram referenced to photons for no light

A102f (43 cameras), FFT saturation 0.5

A102f (43 cameras), FFT saturation 0.5

Figure 9: Spectrogram referenced to photons for 50% saturation

A102f (43 cameras), FFT saturation 0.9

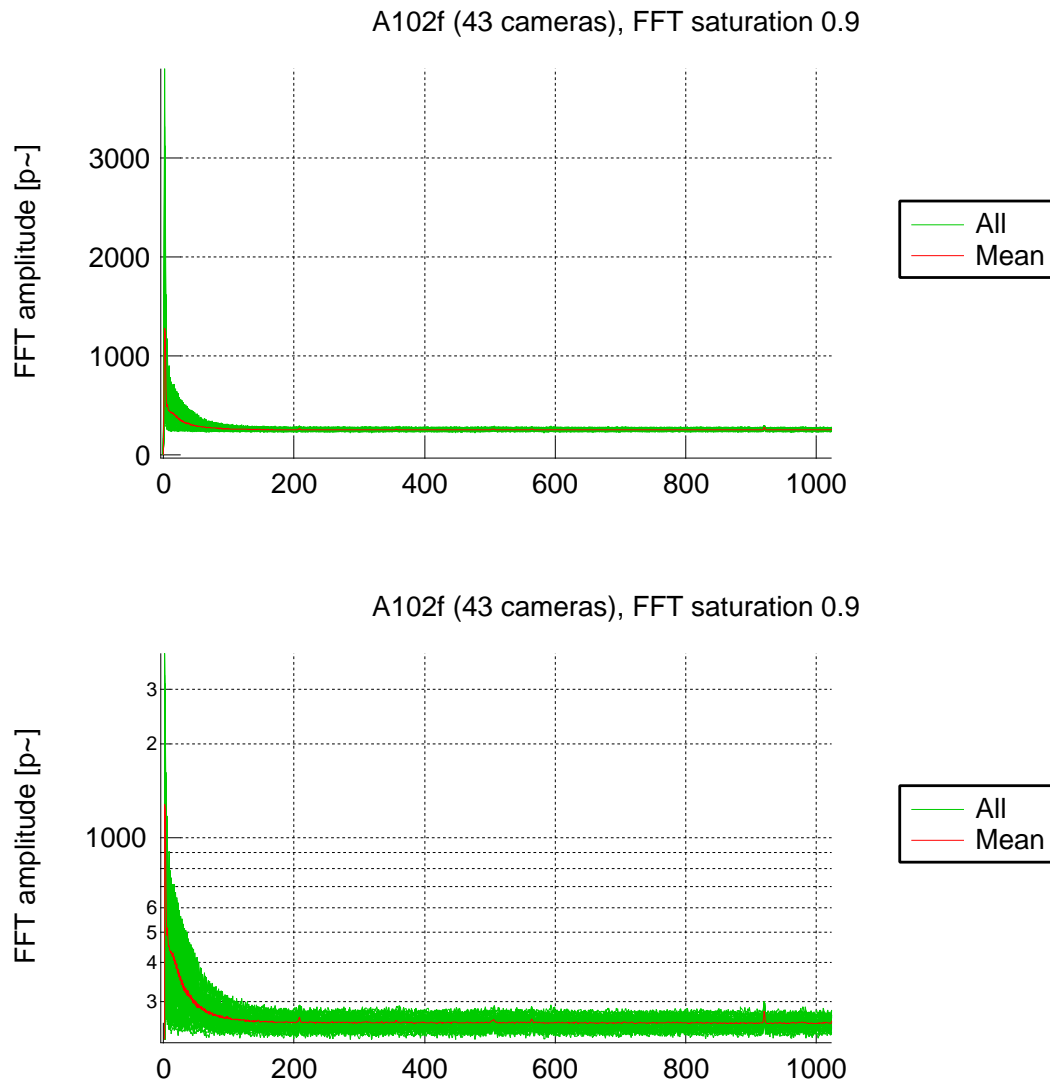A102f (43 cameras), FFT saturation 0.9

Figure 10: Spectrogram referenced to photons for 90% saturation

4.1.9   Non-Whiteness Coefficient

The non-whiteness coefficient is plotted versus the number of photons μ_p in $[p^\sim]$ collected in a pixel during exposure time.
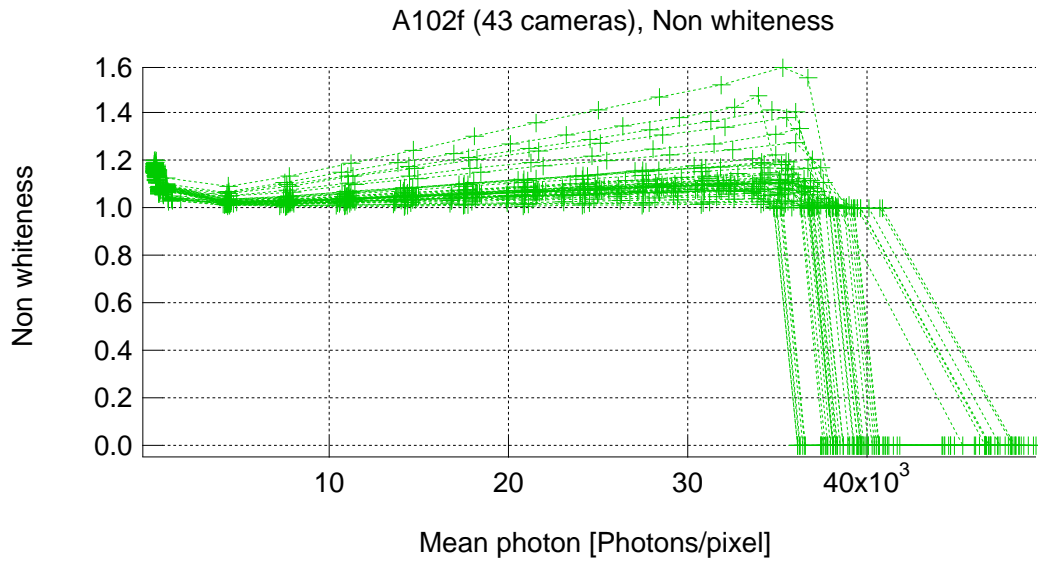

Figure 11: Non-whiteness coefficient

4.2   Derived Data

4.2.1   Absolute sensitivity threshold

Absolute sensitivity threshold $\mu_{p.min}(\lambda)$ in $[\,p^\sim]$ for monochrome light versus wavelength of the light in $[\text{nm}]$.
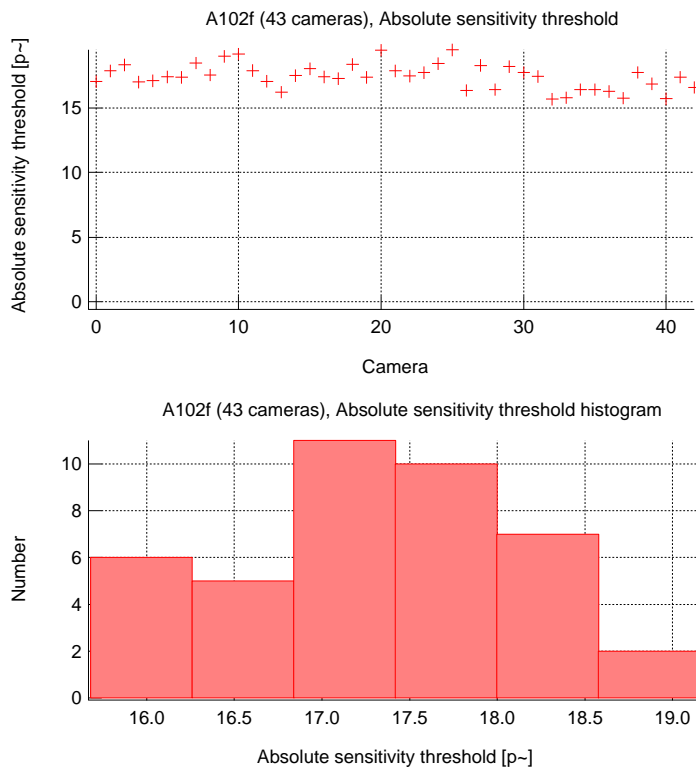
$$\mu_{p.min} = \frac{\sigma_{d_0}}{\eta} \tag{1}$$

Figure 12: Absolute sensitivity threshold

Item	Symbol	Typ.	Std. dev.	Unit	Remarks
Absolute sensitivity threshold	$\mu_{p.min}$	17	TBD	$p^\sim$	$\lambda = 545\,\text{nm}$

Table 10: Absolute sensitivity threshold

4.2.2 Signal to noise ratio

Signal to noise ratio $\text{SNR}_y(\mu_p)$ is plotted versus number of photons μ_p collected in a pixel during exposure time in $[\text{p}^\sim]$ for monochrome light with the wavelength λ given in $[\text{nm}]$. The wavelength should be near the maximum of the quantum efficiency.

$$A : \text{SNR}_y = \frac{\mu_y - \mu_{y.dark}}{\sigma_y} \tag{2}$$

$$B : \text{SNR}_y = \frac{\eta\mu_p}{\sqrt{(\eta\mu_p + \sigma_{d_0}^2)}} \tag{3}$$

Figure 13 shows the signal to noise ratio SNR_y for monochrome light with the wavelength $\lambda = 545\,\text{nm}$.
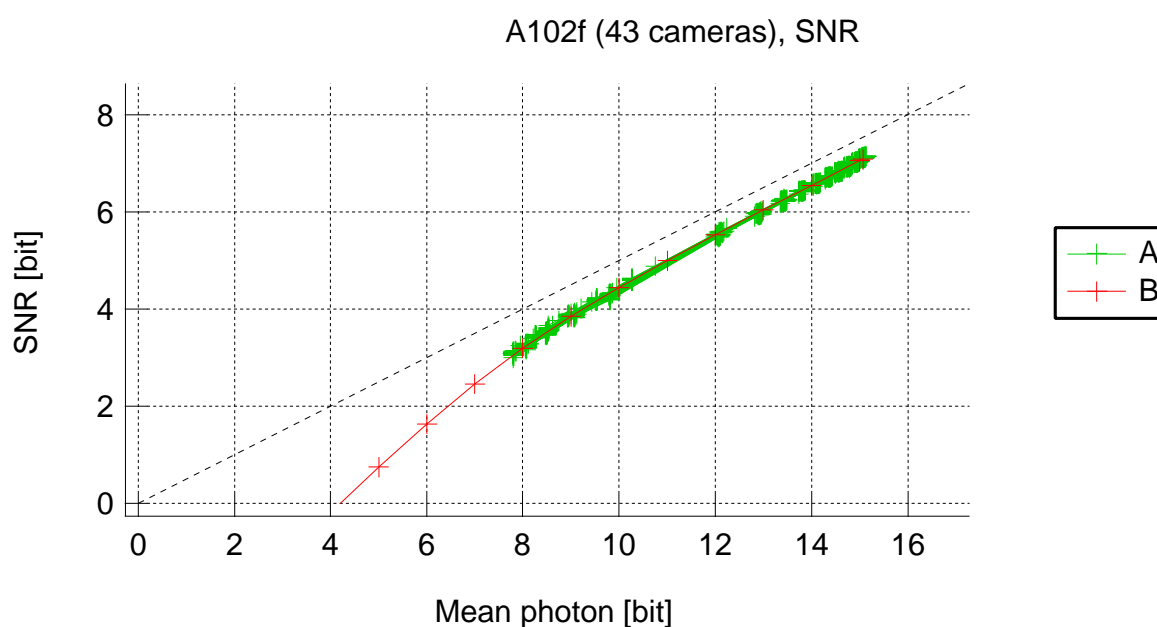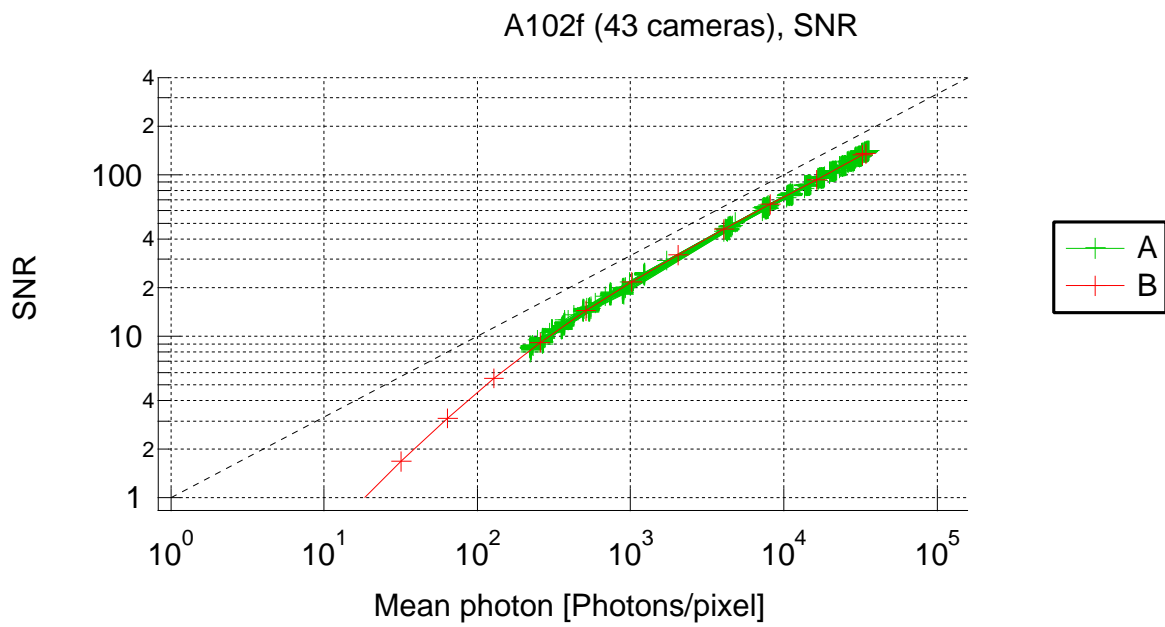

Figure 13: Signal to noise ratio

Figure 14: Signal to noise ratio

4.2.3   Dynamic range

Dynamic range $\text{DYN}_{out.bit}$ in $[\,\text{bit}\,]$.

$$\text{DYN}_{out} = \frac{\mu_{e.sat}}{\sigma_{d_0}} \tag{4}$$

$$\text{DYN}_{out.bit} = \log_2\left(\text{DYN}_{out}\right) \tag{5}$$
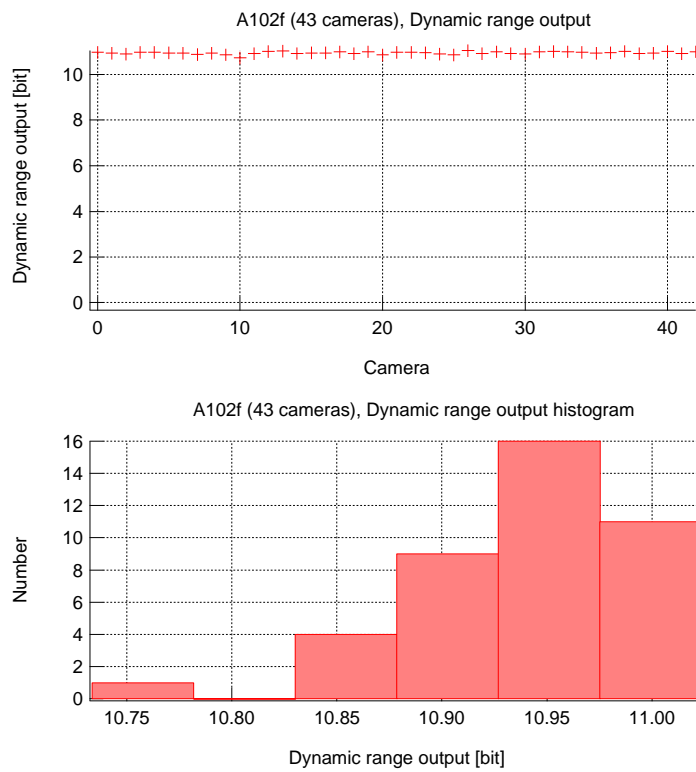
Figure 15: Output dynamic range

Item	Symbol	Typ.	Std. dev.	Unit	Remarks
Output dynamic range	$\text{DYN}_{out.bit}$	10.9	0.06	bit	

Table 11: Output dynamic range

4.3   Raw Measurement Data

4.3.1   Mean gray value

Mean gray value $\mu_y(\mu_p)$ in $[\mathrm{DN}]$ is plotted versus number of photons μ_p in $[\mathrm{p}^\sim]$ collected in a pixel during exposure time.

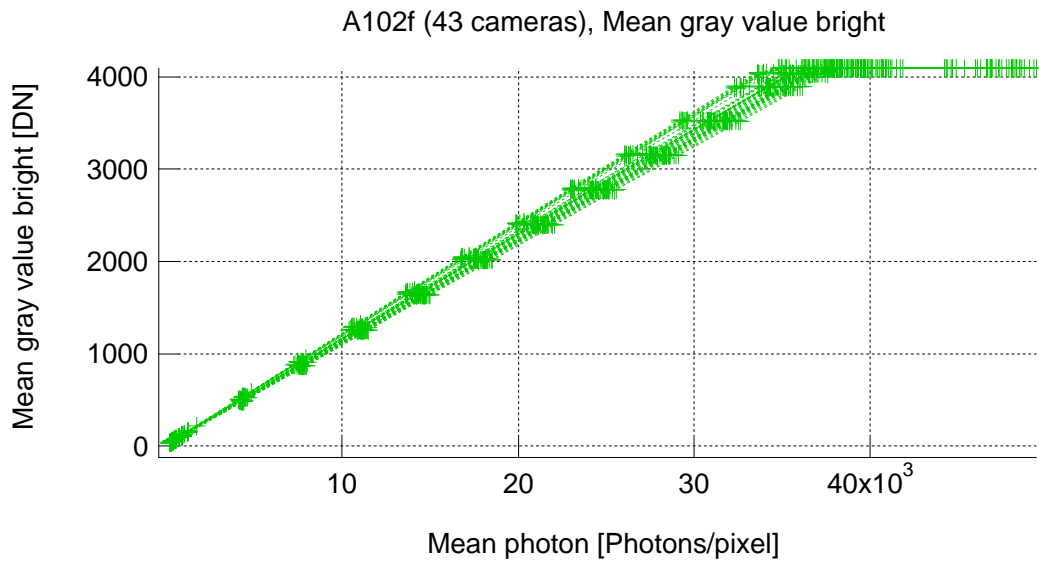A102f (43 cameras), Mean gray value bright

Figure 16: Mean gray values of the cameras with illuminated pixels

4.3.2   Variance of temporal distribution of gray values

Variance of temporal distribution of gray values $\sigma^2_{y.temp}(\mu_p)$ in $[\mathrm{DN}^2]$ is plotted versus number of photons μ_p in $[p^\sim]$ collected in a pixel during exposure time.
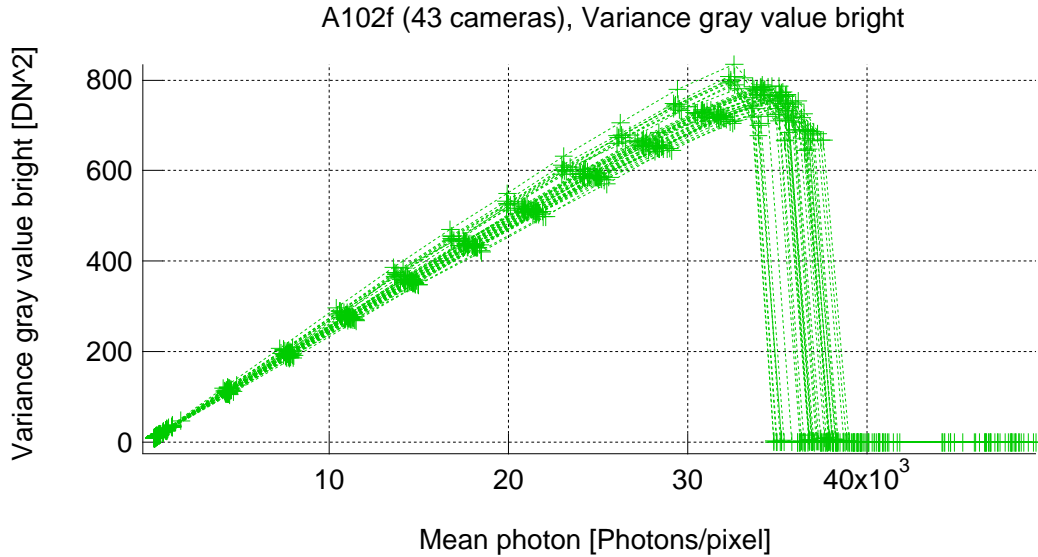

Figure 17: Variance values of temporal distribution of gray values with illuminated pixels

Saturation Capacity   The saturation point is defined as the maximum of the curve in the diagram 17. The abscissa of the maximum point is the number of photons $\mu_{p.sat}$ where the camera saturates. The saturation capacity $\mu_{e.sat}$ in electrons is computed according to the mathematical model as:

$$\mu_{e.sat} = \eta\mu_{p.sat} \tag{6}$$

4.3.3   Mean of the gray values dark signal

Mean of the gray values dark signal $\mu_{y.dark}(T_{exp})$ in $[\mathrm{DN}]$ is plotted versus exposure time in $[\mathrm{s}]$.
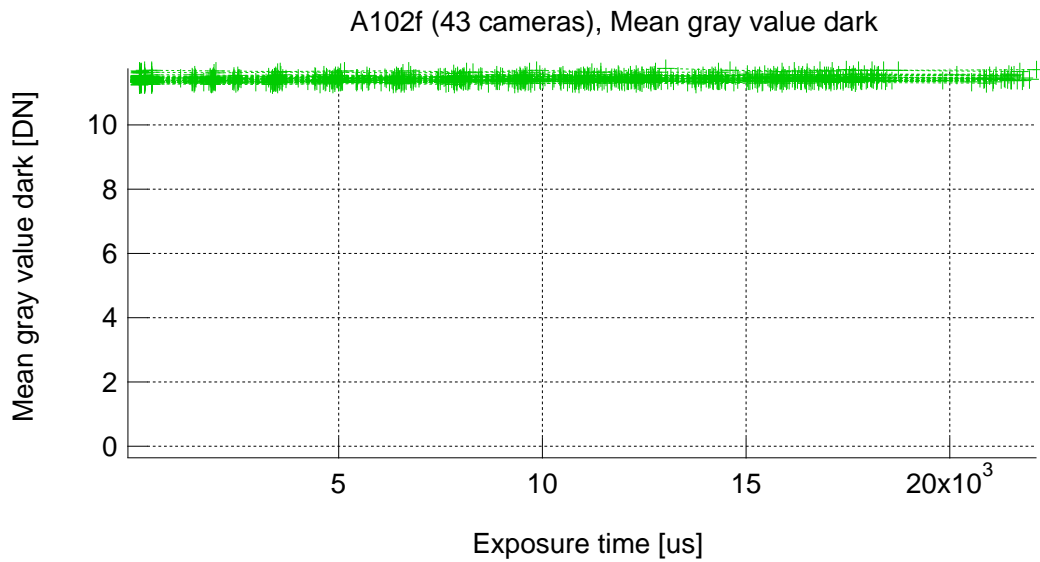

Figure 18: Mean gray values of the cameras in darkness

4.3.4   Variance of the gray values temporal distribution in dark

Variance of the gray values temporal distribution in dark $\sigma^2_{y.temp.dark}(T_{exp})$ in $[\mathrm{DN}^2]$ is plotted versus exposure time T_{exp} in $[\mathrm{s}]$.
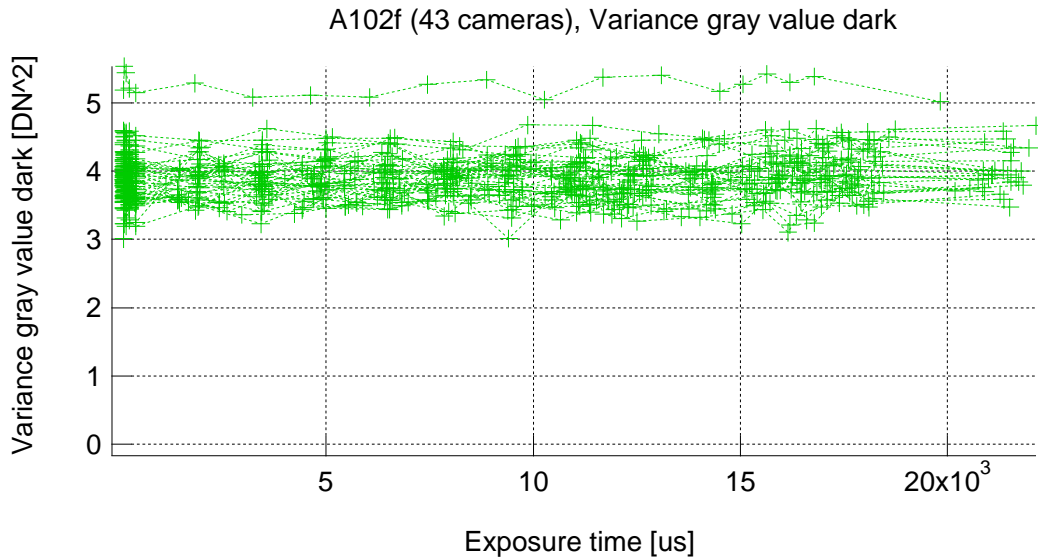

Figure 19: Variance values of temporal distribution of gray values in darkness

Temporal Dark Noise   The dark noise for exposure time zero is found as the offset of the linear correspondence in figure 19. Match a line (with offset) to the linear part of the data in the diagram. The dark noise for exposure time zero $\sigma^2_{d_0}$ is found as the offset of the line divided by the square of the overall system gain K.

$$\sigma_{d_0} = \sqrt{\frac{\sigma^2_{y.temp.dark}(T_{exp} = 0)}{K^2}} \tag{7}$$

4.3.5   Light induced variance of temporal distribution of gray values

The light induced variance of temporal distribution of gray values in $[\mathrm{DN}^2]$ is plotted versus light induced mean gray value in $[\mathrm{DN}]$.
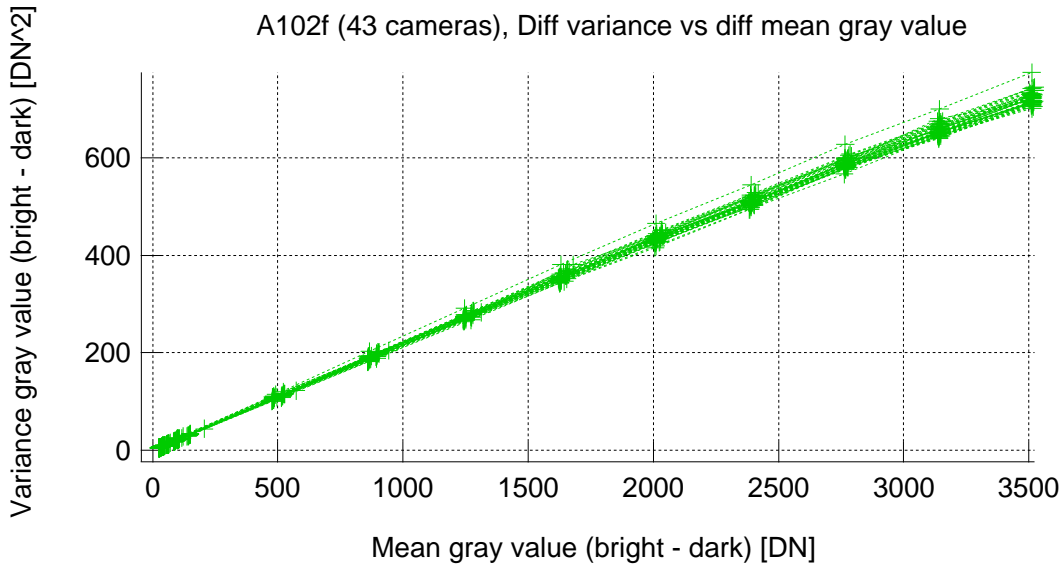

Figure 20: Light induced variance of temporal distribution of gray values versus light induced mean gray value

Overall System Gain   The overall system gain K is computed according to the mathematical model as:

$$K = \frac{\sigma^2_{y.temp} - \sigma^2_{y.temp.dark}}{\mu_y - \mu_{y.dark}} \tag{8}$$

which describes the linear correspondence in the diagram 20. Match a line starting at the origin to the linear part of the data in this diagram. The slope of this line is the overall system gain K.

4.3.6   Light induced mean gray value

The light induced mean gray value $\mu_y - \mu_{y.dark}$ in $[\,\mathrm{DN}\,]$ is plotted versus the number of photons collected in a pixel during exposure time $K\mu_p$ in $[\,\mathrm{p}\,^\sim]$.
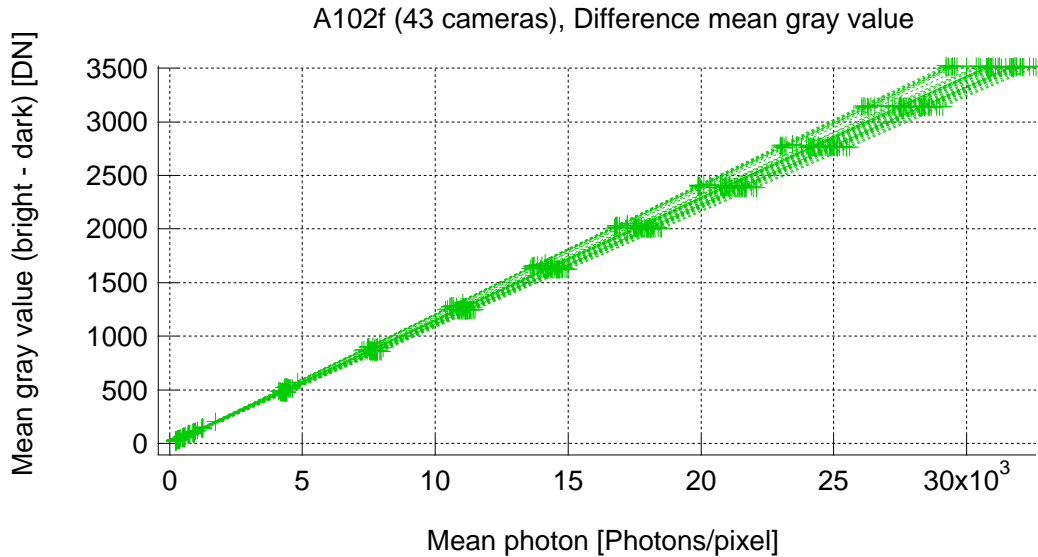

Figure 21: Light induced mean gray value versus the number of photons

Total Quantum Efficiency   The total quantum efficiency η is computed according to the mathematical model as:

$$\eta = \frac{\mu_y - \mu_{y.dark}}{K\mu_p} \tag{9}$$

which describes the linear correspondence in the diagram 21. Match a line starting at the origin to the linear part of the data in this diagram. The slope of this line divided by the overall system gain K yields the total quantum efficiency η.

The number of photons μ_p are calculated using the model for monochrome light. The number of photons Φ_p collected in the geometric pixel per unit exposure time $[\mathrm{p}^\sim/\mathrm{s}]$ is given by

$$\Phi_p = \frac{EA\lambda}{hc} \tag{10}$$

with the irradiance E on the sensor surface $[\mathrm{W/m^2}]$, the area A of the (geometrical) pixel $[\mathrm{m^2}]$, the wavelength λ of light $[\mathrm{m}]$, the Planck's constant $h \approx 6.63 \cdot 10^{-34}\,\mathrm{Js}$ and the speed of light $c \approx 3 \cdot 10^8\,\mathrm{m/s}$. The number of photons can be calculated by

$$\mu_p = \Phi_p T_{exp} \tag{11}$$

during the exposure time T_{exp}. Using equation 9 and the number of photons μ_p, the total quantum efficiency η can be calculated as

$$\eta = \frac{hc}{AT_{exp}} \ \frac{1}{E} \ \frac{1}{\lambda} \ \frac{\mu_p - \mu_{y.dark}}{K}.$$

(12)

4.3.7   Dark current versus housing temperature

Logarithm to the base 2 of the dark current in $[\mathrm{e^-/s}]$ versus deviation of the housing temperature from 30°C in $[\,^\circ\mathrm{C}]$
   Not measured!

5 Characterizing Total and Spatial Noise

5.1 Basic Parameters

5.1.1 Spatial offset noise

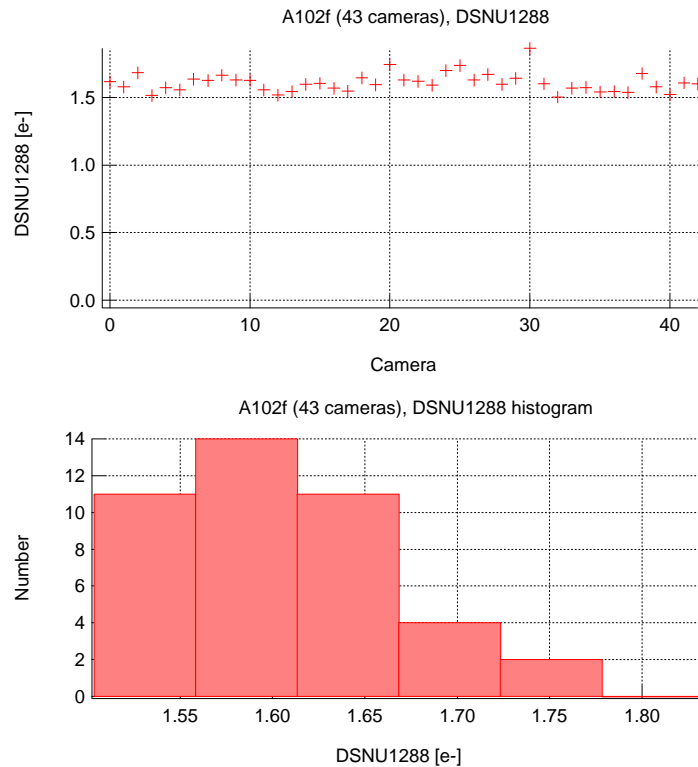Standard deviation of the spatial offset noise σ_o referenced to electrons in $[\mathrm{e}^-]$.

A102f (43 cameras), DSNU1288

A102f (43 cameras), DSNU1288 histogram

Figure 22: Spatial offset noise (DSNU_{1288})

Item	Symbol	Typ.	Std. dev.	Unit	Remarks
Spatial offset noise (DSNU_{1288})	σ_o	1.6	0.1	e^-	

Table 12: Spatial offset noise (DSNU_{1288})

5.1.2   Spatial gain noise
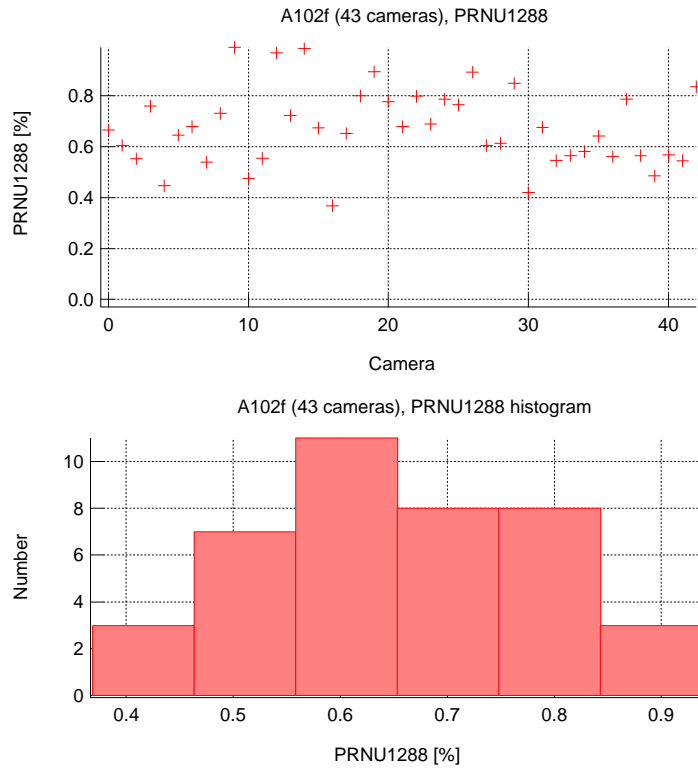
Standard deviation of the spatial gain noise S_g in $[\%]$.

Figure 23: Spatial gain noise (PRNU$_{1288}$)

Item	Symbol	Typ.	Std. dev.	Unit	Remarks
Spatial gain noise (PRNU$_{1288}$)	S_g	0.7	0.2	$\%$	

Table 13: Spatial gain noise (PRNU$_{1288}$)

5.1.3 Spectrogram Spatial Noise

Spectrogram referenced to photons in $[p^\sim]$ is plotted versus spatial frequency in $[1/\text{pixel}]$ for no light, 50% saturation and 90% saturation.
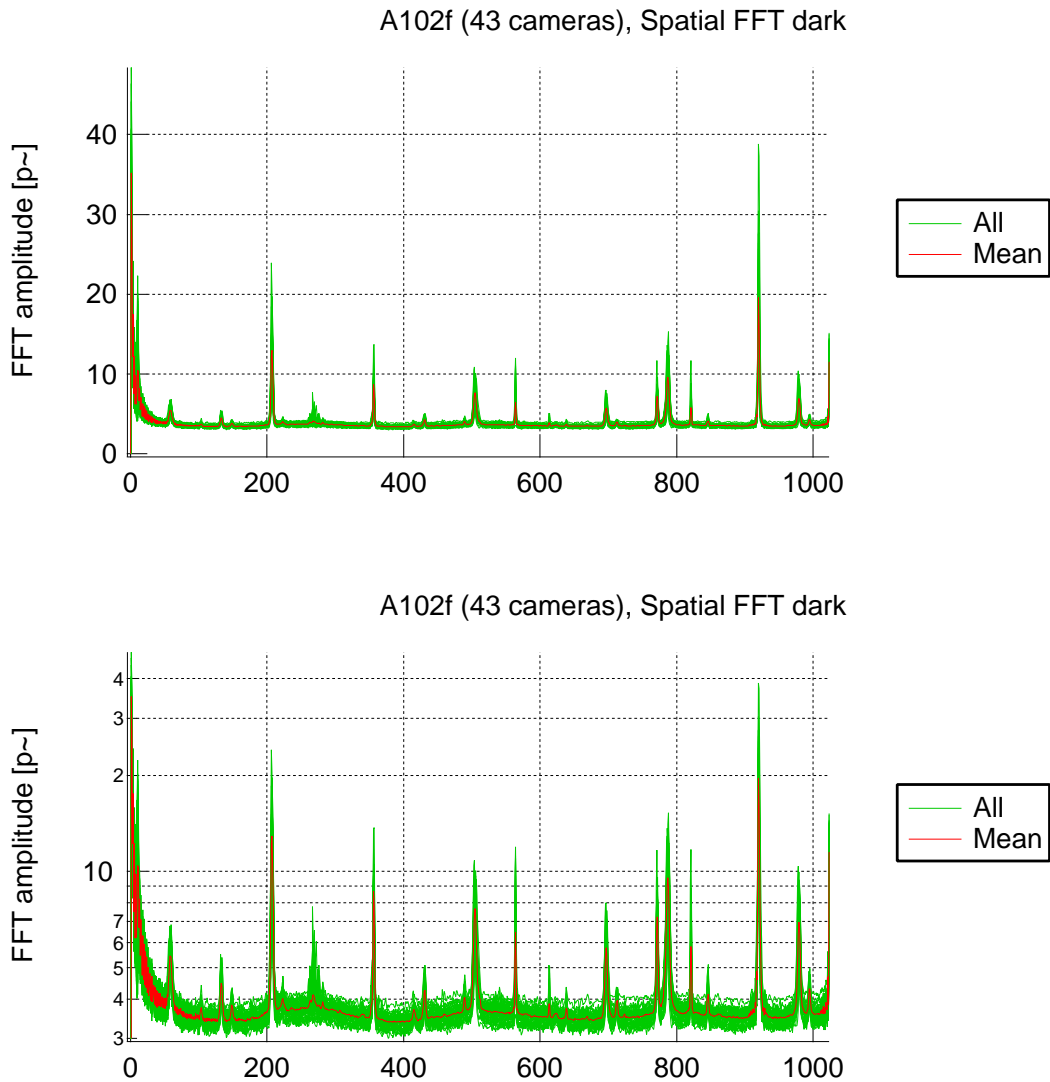
A102f (43 cameras), Spatial FFT dark

A102f (43 cameras), Spatial FFT dark

Figure 24: Spectrogram referenced to photons for no light

A102f (43 cameras), Spatial FFT saturation 0.5

A102f (43 cameras), Spatial FFT saturation 0.5
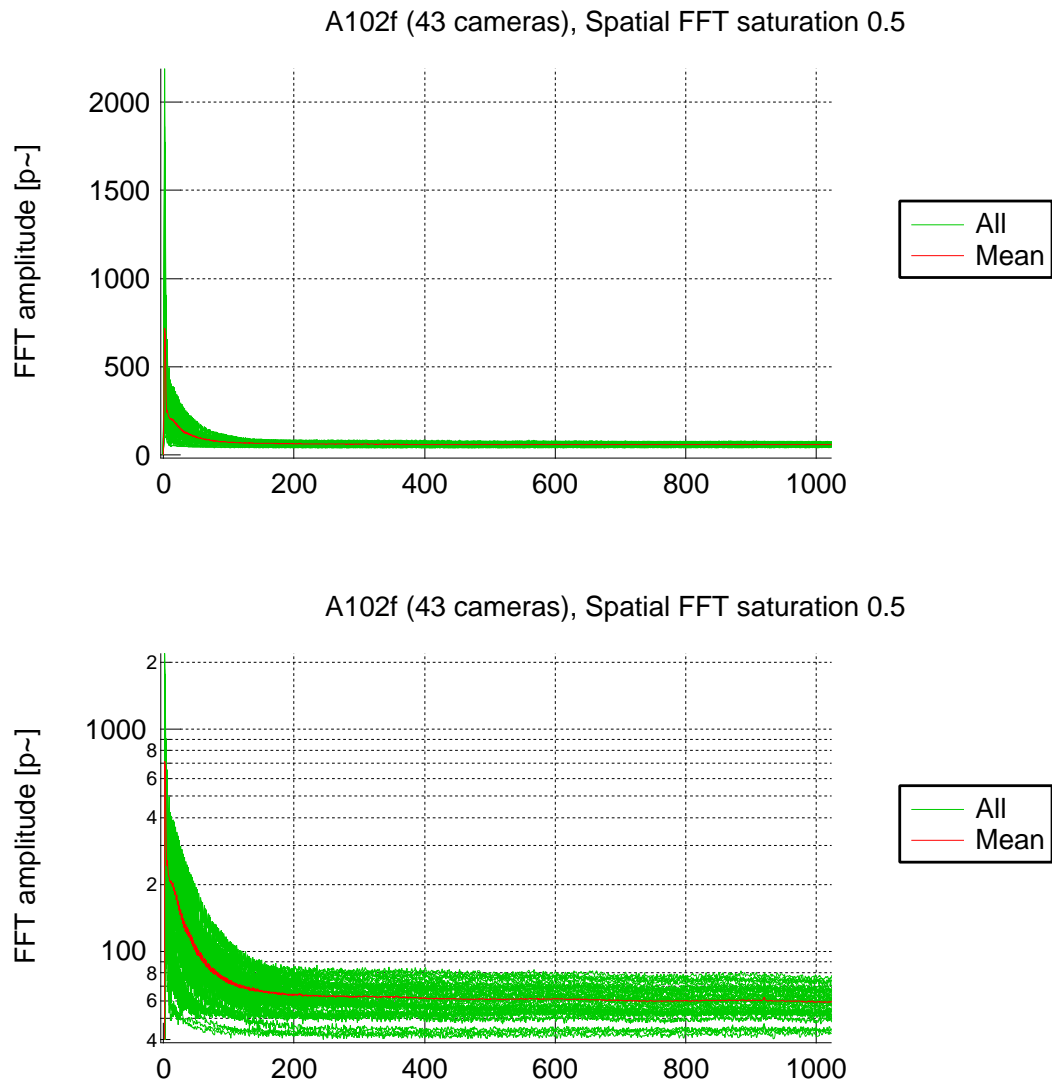
Figure 25: Spectrogram referenced to photons for 50% saturation

A102f (43 cameras), Spatial FFT saturation 0.9

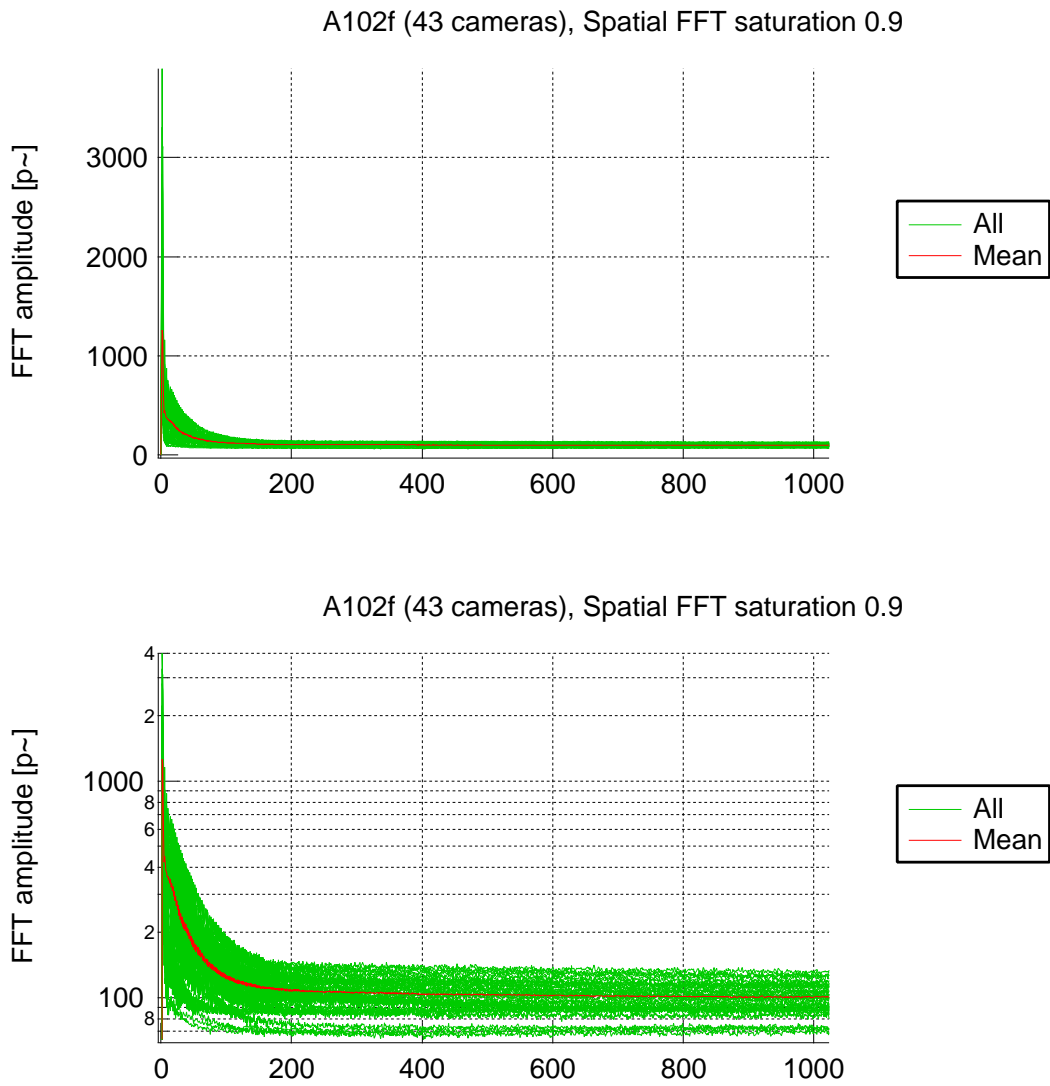A102f (43 cameras), Spatial FFT saturation 0.9

Figure 26: Spectrogram referenced to photons for 90% saturation

5.1.4   Spatial Non-Whiteness Coefficient

The non-whiteness coefficient is plotted versus the number of photons μ_p in $[p^{\sim}]$ collected in a pixel during exposure time.
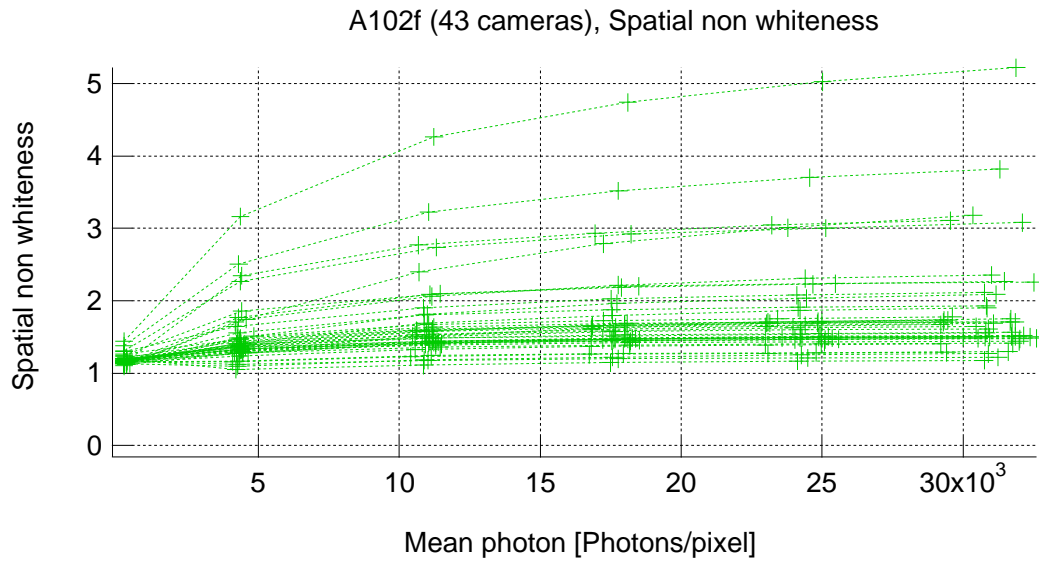

Figure 27: Spatial Non-whiteness coefficient

5.2   Raw Measurement Data

5.2.1   Standard deviation of the spatial dark noise

Standard deviation of the spatial dark noise in $[\mathrm{DN}]$ versus exposure time in $[\mathrm{s}]$.
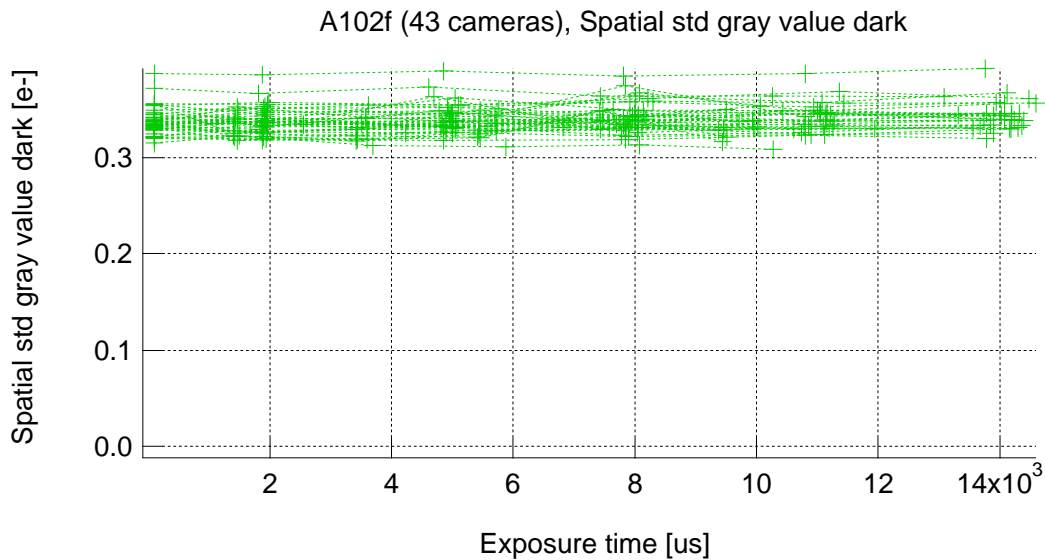
A102f (43 cameras), Spatial std gray value dark

Figure 28: Standard deviation of the spatial dark noise

From the mathematical model, it follows that the **variance of the spatial offset noise** σ_o^2 should be constant and not dependent on the exosure time. Check that the data in the figure 28 forms a flat line. Compute the mean of the values in the diagram. The mean divided by the conversion gain K gives the standard deviation of the spatial offset noise σ_o .

$$\mathrm{DSNU}_{1288} = \sigma_o = \frac{\sigma_{y.spat.dark}}{K} \tag{13}$$

The square of the result equals the variance of the spatial offset noise σ_o^2.

5.2.2   Light induced standard deviation of the spatial noise

Light induced standard deviation of the spatial noise in $[\mathrm{DN}]$ versus light induced mean of gray values $[\mathrm{DN}]$.
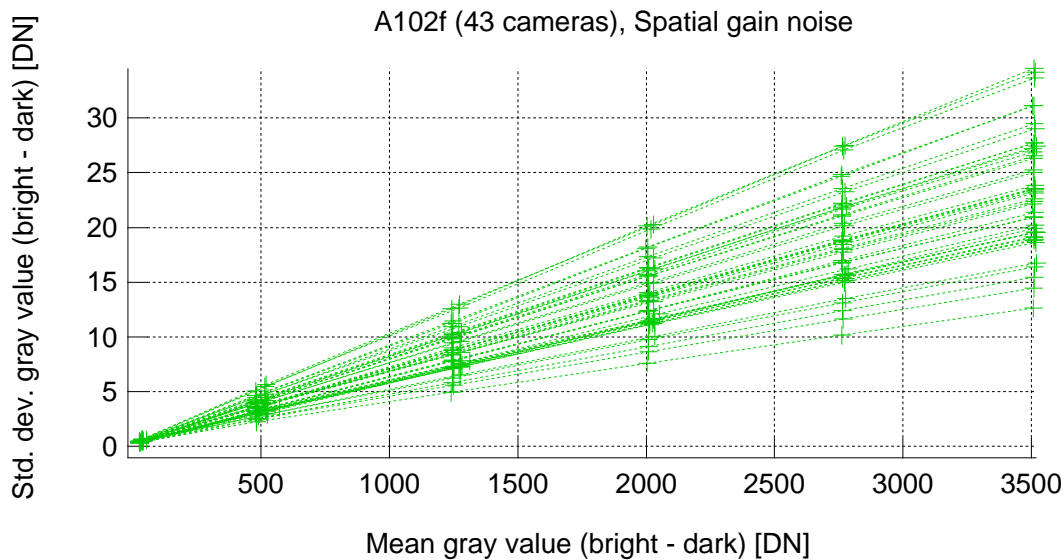

Figure 29: Light induced standard deviation of the spatial noise

The **variance coefficient of the spatial gain noise** S_g^2 or its standard deviation value S_g respectively, is computed according to the mathematical model as

$$\mathrm{PRNU}_{1288} = S_g = \frac{\sqrt{\sigma_{y.spat}^2 - \sigma_{y.spat.dark}^2}}{\mu_y - \mu_{y.dark}}, \tag{14}$$

which describes the linear correspondence in the figure 29. Match a line through the origin to the linear part of the data. The line's slope equals the standard deviation value of the spatial gain noise S_g.

References

[1] EUROPEAN MACHINE VISION ASSOCIATION (EMVA): *EMVA Standard 1288 - Standard for Characterization and Presentation of Specification Data for Image Sensors and Cameras (Release A1.03).* 2006